

Characterization of an Ultrafast Optical Parametric Amplifier System

By Hugh Carney

With the Assistance of Professor Anne Reilly

Contents

I.	Abstract	3
II.	Introduction	4
III.	Background and Theory	6
	A. Ultrafast Lasers	6
	B. Nonlinear Optics	8
	C. Optical Parametric Amplifier	14
IV.	Experimental Methods	16
	A. Set-up	16
	B. Autocorrelation	17
	C. Optical Parametric Amplifier Tuning	20
V.	Results	22
	A. Autocorrelator Results	22
	B. OPA Tuning Results	23
V.	Conclusion	27
VI.	Appendix	28
	A. Appendix 1	28
	B. Appendix 2	29
	C. Appendix 3	30
VII.	References	31

I. Abstract

The purpose of this work is to characterize the optical spectra of an ultrafast optical parametric laser amplifier and measure the temporal pulse width of the ultrafast laser system. An optical parametric amplifier employs nonlinear wave mixing in a crystal to allow tuning over a wide range of wavelengths. This is important for ultrafast laser spectroscopy experiments where tuning to a particular resonance in the material under study is needed. In this work, we are exploring the wavelength tuning and spectra of a Spectra-Physics optical parametric amplifier to characterize it for future spectroscopy experiments.

II. Introduction

Nonlinear optics is a field that has become important since the invention of the laser. It is providing us with a fundamental understanding of the nature of light and revealed to us a world of applications. In the pre-laser era, field strengths of conventional light sources were smaller than the field strength of atomic fields. Observation of nonlinear phenomena would have to wait for new technologies to fill the disparity between the two fields.

The essential property of the laser beam to the development of nonlinear optics is its high degree of coherence. Conventional light sources are made from an enormous number of independently radiating atomic systems that have uncorrelated contributions to a wave field. Laser radiation is characterized by the high degree of ordering of the light field, a degree conventional sources cannot achieve. In such a concentration of energy, both spatially and spectrally, the relationship between the electric polarization P and the field strength E ceases to be linear.

The laser has come a long way from being called “a solution looking for a problem” [1]. Government and industrial laboratories continue to carry out extensive laser research. The Department of Energy has programs on laser driven nuclear fusion [2]. Phone companies have initiated extensive programs to develop semiconductor laser technology to further optical communication [2]. Perhaps most significantly, phone companies have revolutionized communication by sending laser beams through strands of flexible fiber-optic glass that is narrower than a pencil lead. The capacity of the laser is

such that all the signals from telephone, television, radio, and digitalized information could be packed into just one laser beam [1].

Another powerful impact of the laser has been in the area of spectroscopy. Lasers have been used in a vast array of scientific experiments on everything from biological systems to superconductors. The 1999 Nobel Prize in Chemistry was awarded to Ahmed Zewail for the use of ultrafast laser pump-probe techniques to study how chemical reactions occur in real time, with less than a picosecond of resolution.

A state of the art ultrafast laser system has recently been setup in the Physics department at the College. This laser system, consists of a Ti:Sapphire ultrafast laser, a laser amplifier, and an optical parametric amplifier that produces ultrashort pulses (~100 femtoseconds, or $\times 10^{-15}$ sec) and is tunable over a wide range of wavelengths, from 200nm-12,000nm. The system will be used to do pump-probe optical experiments on magnetic materials and high temperature superconductors.

Before the system can be used in this way, however, we must learn how to tune the system and what the output spectra and temporal pulse width of the system is. The goal of this senior project is to begin some of this characterization.

III. Background and Theory

The electromagnetic theory of light is implicit in the relationships among associated electric and magnetic fields. The nonlinear properties of Maxwell's equations are not new. The nonlinear permeability of ferromagnetic media was of prime concern in designing 19th century machinery [3]. However, the beginning of nonlinear optics as a field can be traced to the development of the first working laser by Maiman in 1960. His accomplishment provided the necessary tool.

A. Lasers

The first step towards the development of the laser occurred in 1916, when a paper describing how atoms interact with light by Albert Einstein was published [4]. Einstein theorized that atoms absorbed and emit light in discrete energy packets called photons. He proposed that when an atom was in a high energy level and a photon arrived, it could stimulate the atom to emit another photon of the same energy in a process called stimulated emission. When an atom is stimulated, one photon stimulates an electron to drop to a lower state and emit a photon. One photon goes in and two come out as illustrated in Figure 1.

In 1954, Townes and coworkers developed a device that employs stimulated emissions to generate narrowband microwave radiation from a properly prepared medium, called a MASER (*Microwave Amplification by Stimulated Emission of*

Radiation) [5]. The theory employed in the MASER [6] led to the development of an optical frequency device or laser in 1960.

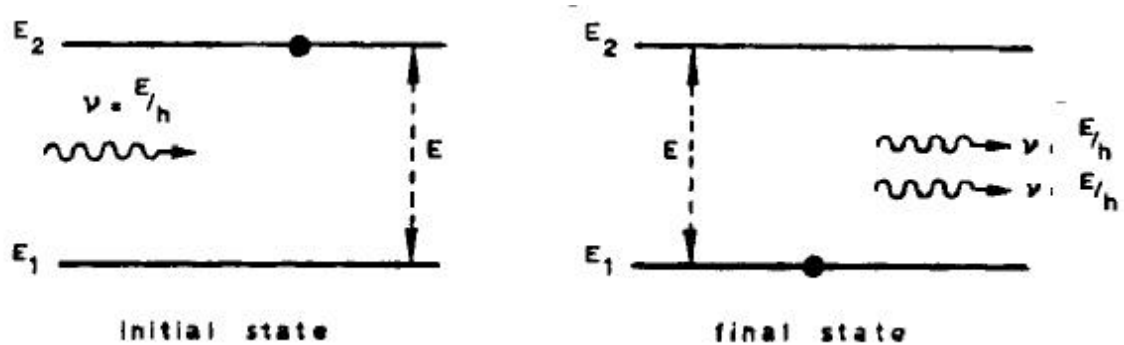


Figure 1: Stimulated Emission (taken from Reference 7)

In stimulated emission, the emitted photon takes off in precisely the same direction as the stimuli light. Stimulated emission results in amplification of a wave at exactly the same frequency and phase called coherent amplification. If an atom is at an excited energy level, more light is emitted than absorbed so the light is stronger [6]. The success of a laser is dependent on material in which the energies of atoms have more excited states than lower states. Therefore, it is necessary to have an incident pump wave with enough intensity to excite at least one half of the ground state atoms. When an electromagnetic wave with the proper frequency is moving through such a material it will pick up energy. The amount of energy picked up on one pass through the material will not be large so a laser must send it through many times. This can be done by the reflective surfaces of two mirrors at the end of the cavity to reflect the wave back and forth. The amount of energy accumulated within this system can be destructive so one of the mirrors has to be made slightly transparent. As a result, a coherent beam of radiation,

produced from light amplification by stimulated emission, emerges (see Appendix 1). This coherent beam is a constant wave laser.

A pulsed laser has a lasing process similar to that of a constant wave laser, however, its output consists of light pulses with a certain duration (anywhere from microseconds to tens of femtoseconds). A pulsed laser can be made either by mixing together waves in the cavity which have different frequencies or by trapping the energy in the cavity and dumping it all out at once in a process call Q-switching. The laser is pulsed when the cavity is allowed to become partially leaky, letting out some of the photons. The result is a series of pulses that stream out of the laser instead of a constant wave. The temporal width of a pulse and the output spectrum of the laser can be related through the Heisenberg uncertainty relationship $\Delta\nu\Delta t \geq K$. For a constant wave laser, $\Delta\nu$ is essentially, though not exactly, 0. For a pulsed laser, the spectral width can be large, as high as tens of nanometers. For a pulse with a Gaussian shape, $K=0.441$ [7].

B. Nonlinear Optics

Franken and his staff observed the first nonlinear optical properties in 1961 [5]. A ruby laser with the wavelength $\lambda=6943\text{\AA}$ and the average power to the order of 10kW was focused on a quartz crystal. The light transmitted was passed through a filter that removed the red light and allowed ultraviolet light to pass and was detected by a photodetector. Radiation with wavelength $\lambda=3471\text{\AA}$ and the power of the order 1mW was observed in the transmitted light. Franken had observed second harmonic generation, that is, a doubling of the frequency of the light.

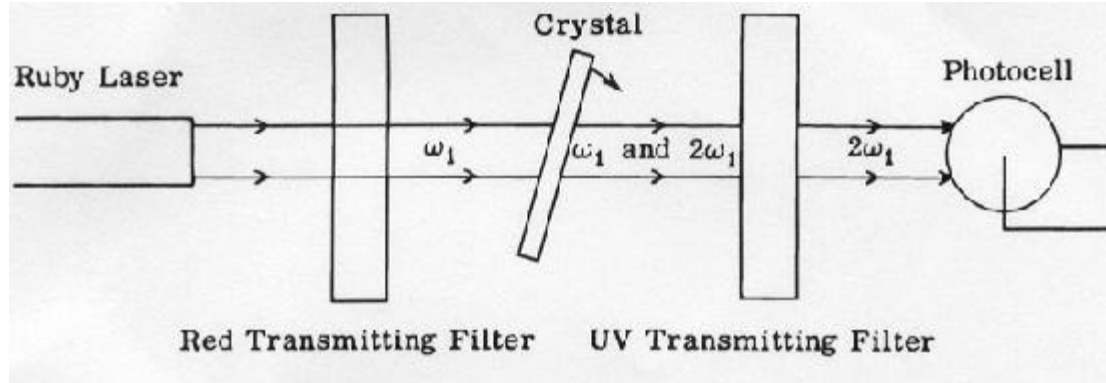


Figure 2: Setup Used by Franken (taken from Reference 5)

Both linear and nonlinear optical phenomena can be described by Maxwell's equations. Maxwell's equations describe the basic laws of an electric field E and magnetic field B of a light wave incident on a medium [7]:

$$\nabla \times E = -\frac{1}{c} \frac{\partial B}{\partial t} \quad (1)$$

$$\nabla \cdot B = 0 \quad (2)$$

$$\nabla \times H = \frac{1}{c} \frac{\partial D}{\partial t} + \frac{4\mathbf{p}}{c} J \quad (3)$$

$$\nabla \cdot D = 4\pi \mathbf{p} \quad (4)$$

If we assume that the material is nonconducting and nonmagnetic, then $\sigma=0$. The electric displacement vector is given by $D=E+4\pi P$ and $B=H$. The vector polarization response [8] is:

$$P(r,t) = \int_{-\infty}^t J(r,t') dt' \quad (5)$$

An additional relationship between the optical response of the medium and the wave fields is needed to sufficiently describe the propagation of light. This relation takes the form

$$P = P(E, B) \quad (6)$$

Because we are not considering magnetized media this reduces to

$$P = P(E) \quad (7)$$

When a dielectric medium is placed in an electric field it is polarized. Each molecule acts as a dipole with dipole moment p_i . The dipole moment vector is then given by

$$P = \sum_i p_i \quad (8)$$

Where the summation is over the dipoles in the unit of volume. Both the properties of the medium and the field strength determine the orienting effect of the external field on the molecular dipoles [5]. Taking this into account the equation changes to

$$P = \sum_i \epsilon_0 \chi E \quad (9)$$

Where χ is the dielectric susceptibility of the medium and ϵ_0 is the permittivity of free space. This polarization is completely linear; for a field increase of a factor of ten the polarization increases by the same factor. This will only be valid for limited values of the field strength.

With a sufficiently large electric field, nonlinear optical responses arise. One can visualize the subatomic fields exhibiting a restoring force that is linearly proportional to the applied force similar to a spring. A laser will push this spring past its elastic limits causing a nonlinear response in the system. The new polarization can be described by:

$$P = P^{(1)} + P^{(2)} + P^{(3)} + \dots \quad (10)$$

$$P = \epsilon_0(\chi^{(1)}E + \chi^{(2)}E^2 + \chi^{(3)}E^3 + \dots) \quad (11)$$

If the fields are low then only the first term of Equation 10 and 11 remain. $\chi^{(2)}$, $\chi^{(3)}$ and the other higher order terms, are called nonlinear susceptibilities and define the degree of nonlinearity. The larger the electric field, the more significant these terms are.

$P^{(2)} = \chi^{(2)}E^2$ is the second order nonlinear polarization and it is used to convert the output of a fixed frequency laser into a different spectral region. Suppose that a single electromagnetic field of frequency ω incidents on a nonlinear medium has the form $E = E_0 \cos \omega t$. That would make the second order nonlinear polarization:

$$P^{(2)} = \epsilon_0 \chi^{(2)} E_0^2 \cos^2 \omega t \quad (12)$$

Using the trigonometric relations $\cos 2x = \cos^2 x - \sin^2 x = 2\cos^2 x - 1$, this equation can be rewritten:

$$P^{(2)} = \frac{1}{2} \epsilon_0 \chi^{(2)} E_0^2 + \frac{1}{2} \epsilon_0 \chi^{(2)} E_0^2 \cos 2\omega t \quad (13)$$

The first term is a constant; it gives rise to a dc field across the medium. The second oscillates at the frequency 2ω . This is illustrated in the schematic below:

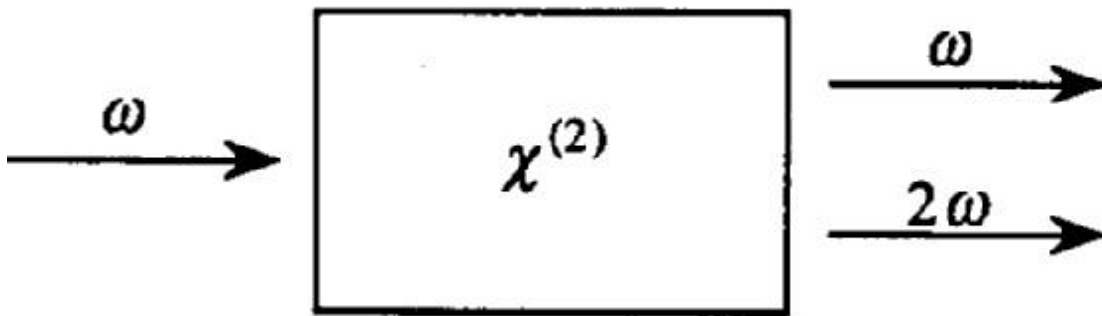


Figure 3: SHG Process (taken from Reference 7)

Second Harmonic Generation can be visualized in terms of the exchange of photons between the frequency components of the field. In this view two photons of frequency ω are destroyed while simultaneously a photon with frequency 2ω is created [9]. This quantum mechanical process is illustrated in the energy level diagram below.

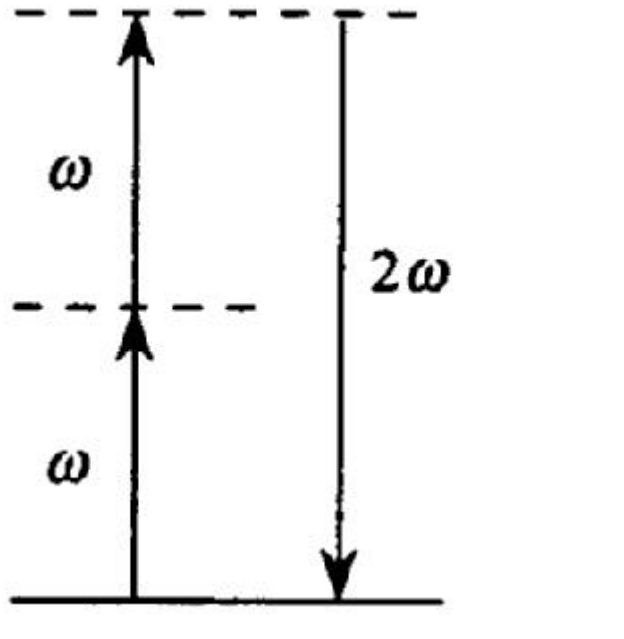


Figure 4: SHG Energy Diagram (taken from Reference 7)

When two beams of different frequencies (ω_1 and ω_2) are passed through a nonlinear crystal additional nonlinear effects can be observed. Sum frequency generation is given by

$$P(\omega_1 + \omega_2) = 2\mathbf{c}^{(2)} E_1 E_2 \quad (14)$$

when there are two input waves of different frequencies. The geometry of interaction and the energy level description are shown below.

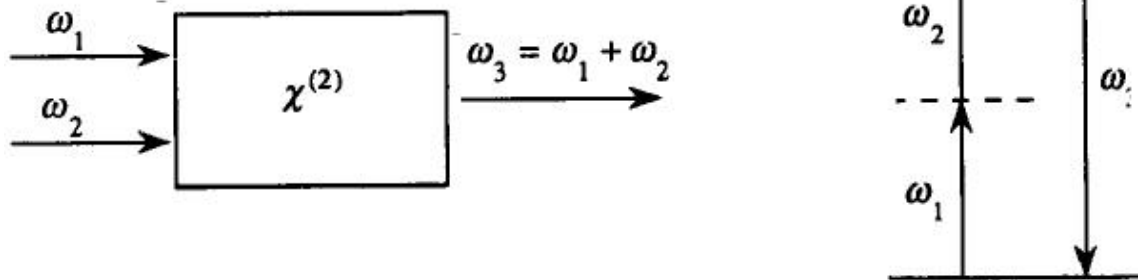


Figure 5: Sum Frequency Generation (taken from Reference 7)

In a like manner difference frequency generations are given by

$$P(\omega_1 - \omega_2) = 2c^{(2)} E_1 E_2^* \quad (16)$$

The important difference is seen in the energy level descriptions where an atom absorbs a photon of frequency ω_1 and then releases two photons of frequency ω_2 and ω_3 .

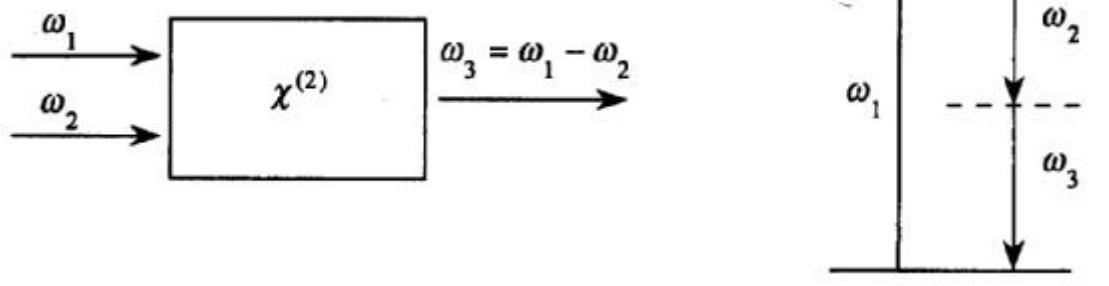


Figure 6: Difference Frequency Generation (taken from Reference 7)

Many material have a nonlinear response, but crystals are used most often because they can have large nonlinear responses due to their structure. The nonlinear response can be calculated either quantum mechanically or estimated using a classical anharmonic oscillator model [7]. An important feature in determining the nonlinear response is a condition known as phase matching. Any material is made up of an enormous number of atomic dipoles that oscillate at a phase that is determined by the

phases of the incoming beam. The relative phasing of these dipoles can be manipulated so that the field radiated by each dipole will add constructively to the incident beam. This means that a crystal must be oriented in a particular manner relative to the incident beams for a particular nonlinear response to occur. It also means that fields from various processes (SHG, for example) will have k vectors in specific directions.

C. Optical Parametric Amplification

Optical parametric amplification is an instantaneous process in which excitation and emission occur without time delay. A nonlinear crystal with second order susceptibility is excited with an intense pump beam with n_2 photons at angular frequency ω_2 . At the same time a weak signal pulse containing n_1 photons at angular frequency ω_1 also incidents on the crystal. As long as $\omega_1 < \omega_2$, then an Optical Parametric Amplifier system can derive gain at the phase-matched condition from nonlinear sum generation [10]. In an OPA system, a larger pump beam amplifies a weak incoming signal, one photon with angular frequency ω_2 destroyed while two photons are created. One of the new photons has the signal frequency $\omega_1(n_1+1)$ and the other has the new frequency $\omega_3(n_3+1)$, such that $\omega_2 = \omega_1 + \omega_3$ [12]. This process leads to an increase in the signal photon flux and therefore the amplification of the signal beam. One application of an OPA system is that its output can be tuned in wavelength, by rotating the orientation of the nonlinear crystal and changing the phase-matching condition.

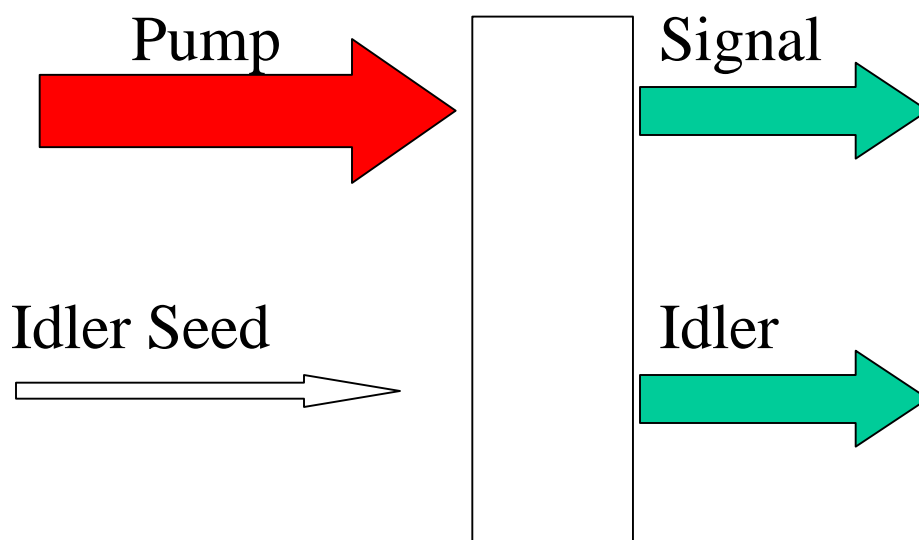


Figure 7: OPA System (taken from Spectra-Physics OPA Manual)

IV. Experimental Methods

A. Laser Set-up

The laser setup that was characterized consisted of a Spectra-Physics Millennia V diode-pumped crystal laser that generates 5 watts of green light that pumps a Tsunami Titanium-doped sapphire laser with output of approximately 150 femtosecond pulses at 800nm. The Ti:Sapphire beam is then directed into the Spitfire Ti:Sapphire regenerative amplifier for amplification. In this setup the Ti:Sapphire provides the seed for the Spitfire Ti:Sapphire regenerative amplifier system. The driver for the amplification process in the Spitfire is a frequency doubled Diode-pumped Nd:YLF laser. The Spitfire amplifies the original seed pulses by a million times from 1nJ of energy per pulse to 1mJ per pulse.

Bright beams have the tendency to self-focus destructively because of the nonlinearity in the index of refraction. This limits the intensity present in amplifiers to less than $10\text{GW}/\text{cm}^2$. The Spitfire finds its way around this by stretching the duration of the pulse and thus reducing its self-focusing induced damage significantly. Using a series of gratings stretches the pulse. This pulse is then amplified and recompressed to its original duration.

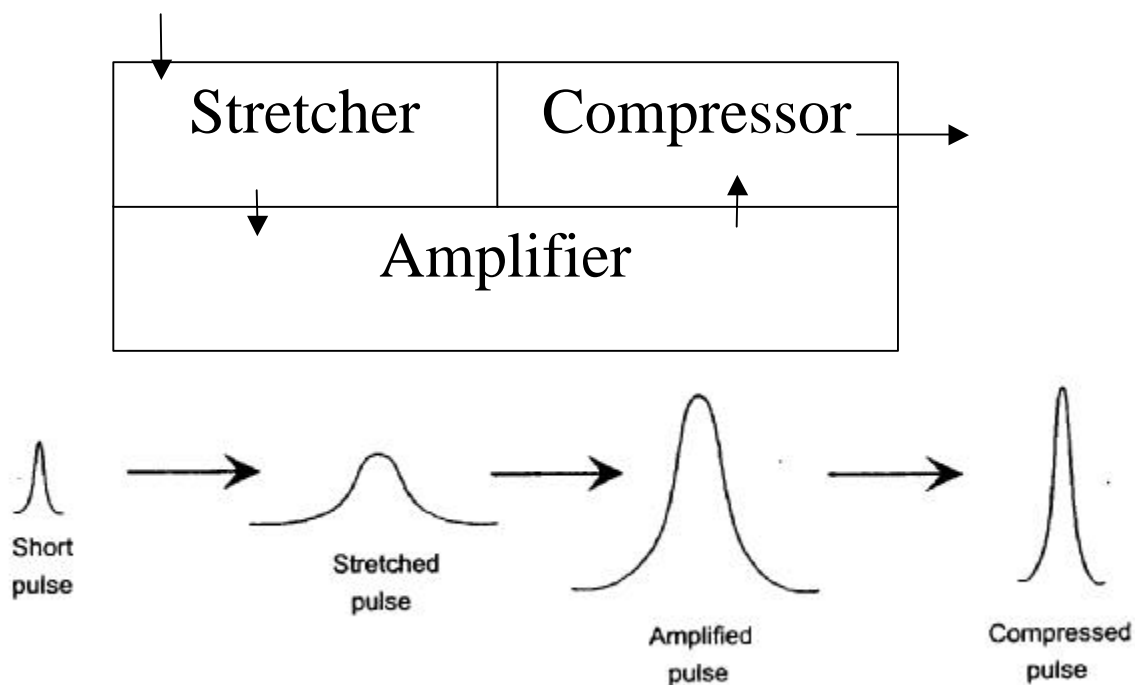


Figure 8: The Spitfire Amplification Process (lower part taken from Spitfire manual)

The final piece of the laser setup is the Optical Parametric Amplifier (OPA). The amplified Ti:Saph laser enters the (OPA) system, where it is split into two beams: a pump and a signal beam. The intense pump beam is used to amplify a low energy seed beam as shown previously.

The laser setup for autocorrelation is shown in Appendix 2 and the laser setup for gathering OPA spectra is shown in Appendix 3.

B. Autocorrelation

Autocorrelation was used to find the ultrafast pulse width of an amplified Ti:Saph beam. Using this method two beams must overlap in time and space. Both beams originate from the same source, a single amplified Ti:Saph beam from the Spitfire. This

single beam is passed through a beam splitter that reflects 50% and transmits 50% as seen below.

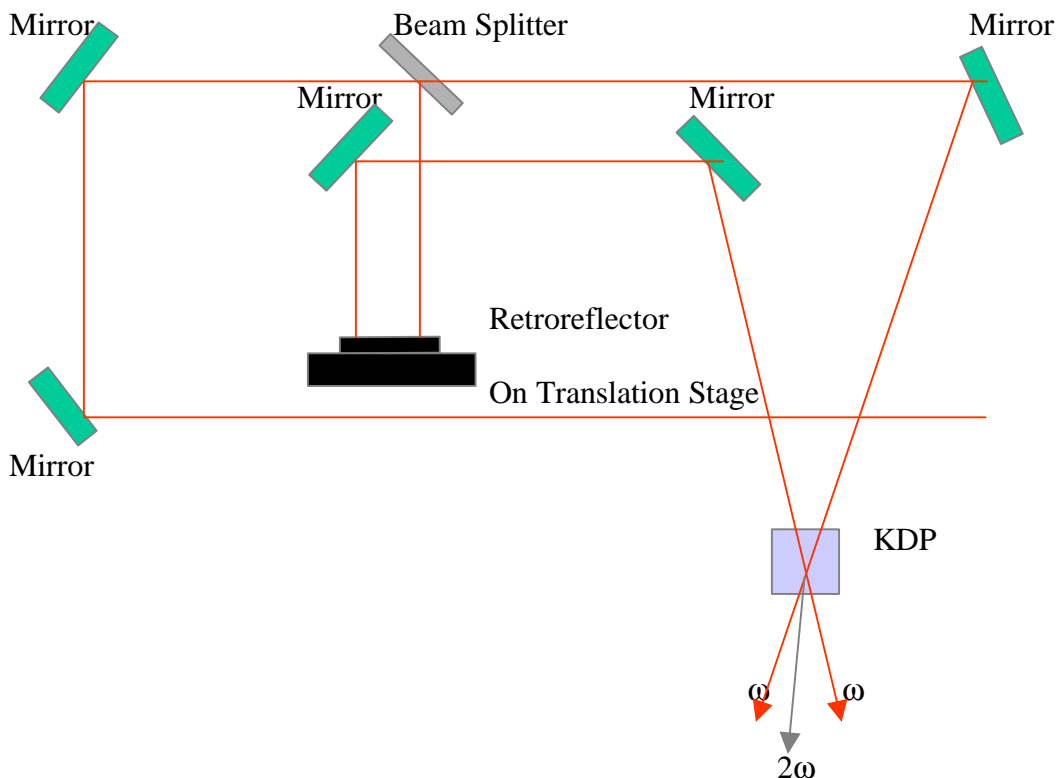


Figure 9: Autocorrelation setup

The portion of the beam that is allowed through the splitter unimpeded is then reflected of a single mirror that then reflects it towards the crystal. This beams path is a set path that must remain a constant length through the experiment.

The second beam path is not a constant length. After reflection, the second beam is reflected on a series of mirrors that take it to retroreflector that is mounted on a translation stage. A retroreflector uses a series of angled mirrors to reflect an incoming beam in the opposite direction only to the side as shown below.

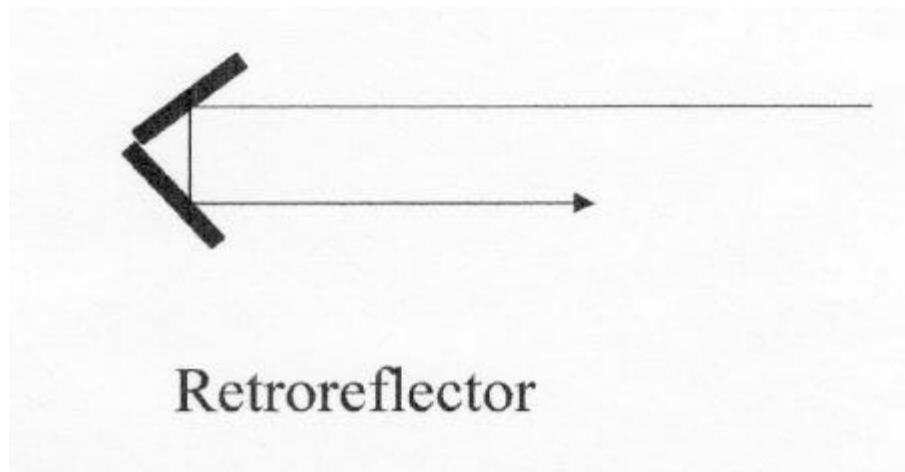


Figure 10

The retroreflector sits on top of a translation stage. The translation stage gives experimenters the ability to lengthen or shorten the distance the beam is taking, providing various delay times between the pulses. Because the amplified beams have such high power, a lens is not needed to focus the beams onto the crystal.

Three conditions must be met to find the zero-delay condition that generates a sum frequency second harmonic generation: First, the two beams must be on the same area within the crystal so that they overlap; second, the angle of the crystal must be exactly in-between the angles that generate SHG for the two single beams; third, the two path lengths must be the same length or the pulses must overlap in time.

After the two beams are focused on the crystal so that they overlap inside the crystal, then the crystal is adjusted to the approximate appropriate angle (phase matching angle). Then the translations stage is moved altering the path length of one of the beams. Because the angle of the crystal is an approximation, the angle must be slightly adjusted and the translation stage moved again until a second harmonic generation beam is observed.

If the two beams have the exact same path length and are focused on the same area of the crystal then they will overlap in both time and space. When this occurs the two beams meet the zero-delay condition and a beam twice the frequency should be seen emerging between the two focused contributing beams. This sum frequency beam should have a low enough intensity to be measured by a photomultiplier tube (PMT), although one was effectively destroyed when using the amplified beam as the source beam. Data from the autocorrelation method was taken and is conveyed by plotting the intensity of the light versus the position of the translation stage. The resulting plot traces out the temporal shape of either pulse. The auto correlation is described by this equation [12]:

$$G_2(\mathbf{t}) = \frac{\int I(t)I(t - \mathbf{t})dt}{\int I^2 dt} \quad (17)$$

Where $I(t)$ is the intensity of beam 1, and $I(t - \mathbf{t})$ is the intensity of the delayed beam 2.

C. Gathering Optical Parametric Amplifier Spectra

The amplified signal and idler output wavelengths are determined by the phase-matching angle of the BBO crystal inside the OPA system. To characterize the laser spectrum we manually turn the crystal to tune the OPA beam to a particular wavelength region. The infrared region of the spectrum is accessed by passing this light through a crystal and performing difference frequency mixing (DFM). A McPherson .3 meter scanning monochromator measured the spectrum. The grating inside the Monochromator is 75 grooves/mm. A stepper motor that is controlled by a Labview program turned the grating allowing the OPA spectrum to be observed. The grating separates the light into

its underlying components. The red components of light no longer have the same optical path as the blue components as shown below.

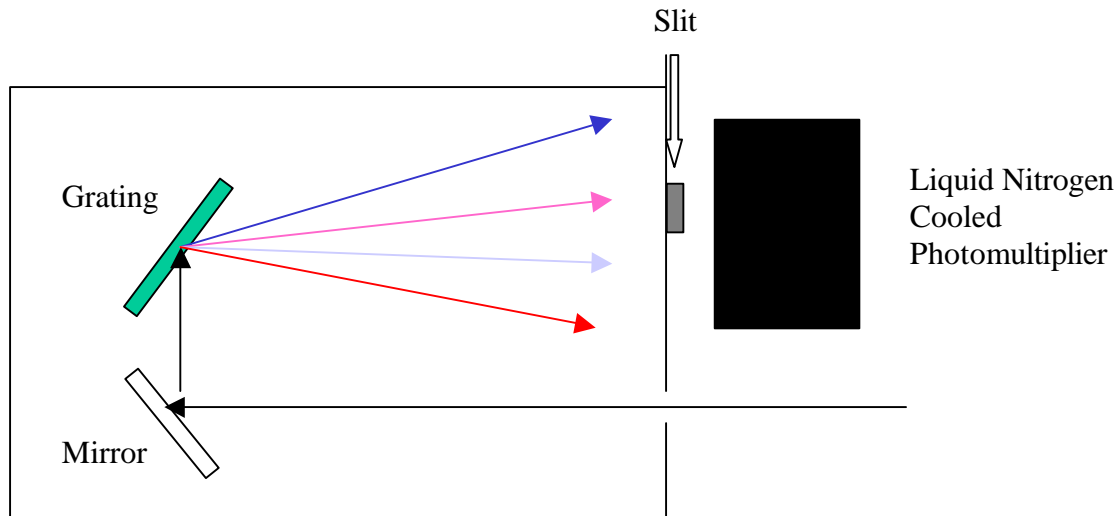


Figure 11: Inside of Monochromator the grating divides the light into it's principle parts

A slit separates out a small component of the spectrum, which is then sent into a liquid nitrogen cooled photomultiplier tube. By physically rotating the grating the spectrum is scanned. A computer measures the output of the detector. The amount of light that is detected by the photomultiplier is dependent on the width of the slit opening. It is very important to know the monochromator starting point so that wavelength can be calculated. This is usually done using a reference light, such as a mercury lamp.

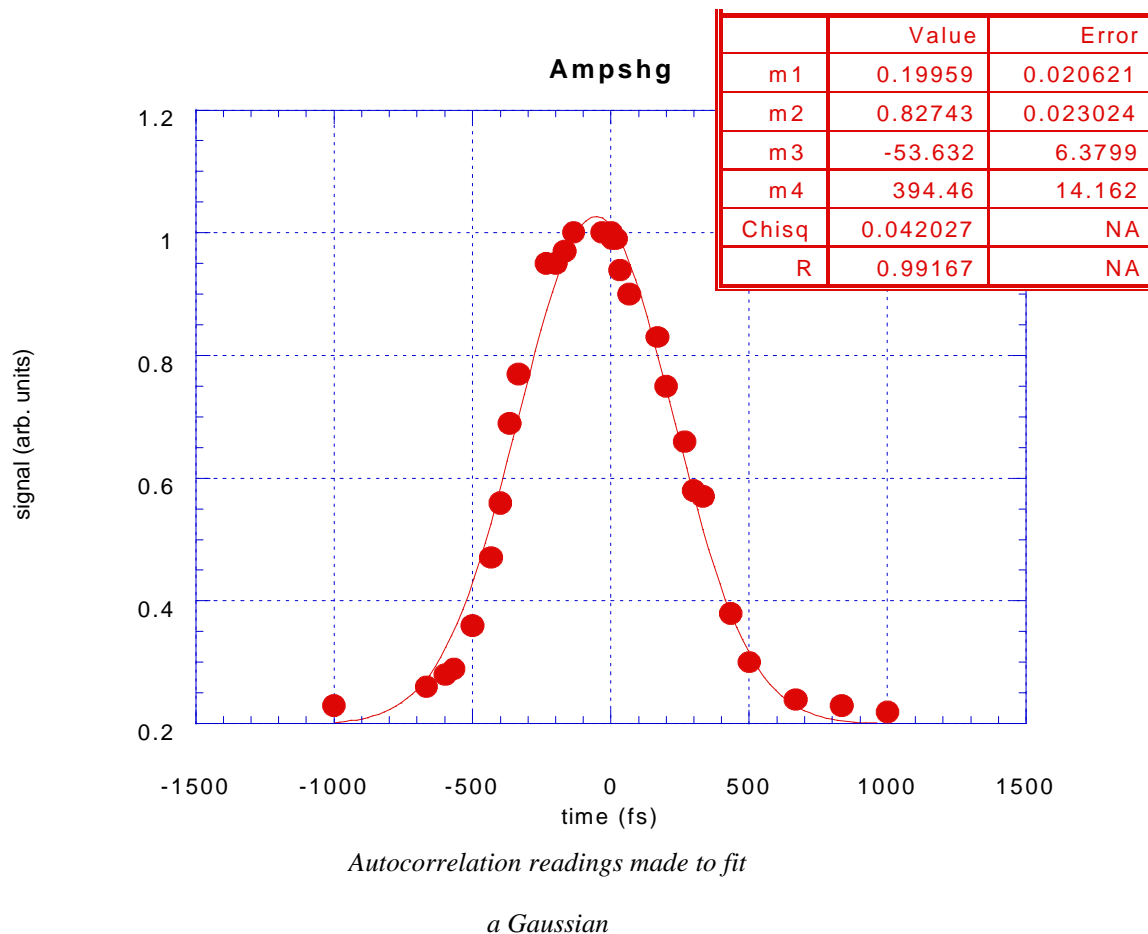
V. Results

A. Autocorrelation Results

Data was recorded from a photomultiplier tube versus the micrometer reading on the translation stage. The micrometer settings were then converted into delay time using the relationship $d=ct$ (d =distance, c =speed of light, t =time). Kaleidoscope was used to plot the data and the points were fit to a Gaussian curve given by:

$$m_1 + m_2 e^{-\frac{(m_0 - m_3)^2}{m_4^2}} \quad (18)$$

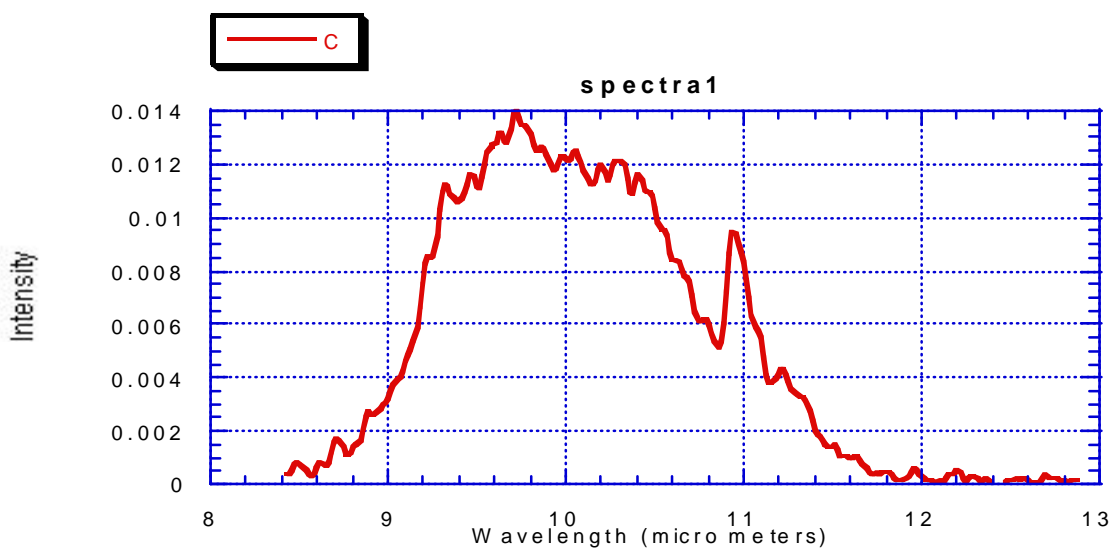
The peak of this curve was defined to be the zero-delay setting.



The width from this Gaussian fit was found to be 395 femtoseconds. This is much larger than 150 femtoseconds expected from the laser system. This means that the pulse is being broadened, either in the amplifier by improper alignment of optical elements, or the use of optical elements to measure the beam which are inappropriately broadening the width.

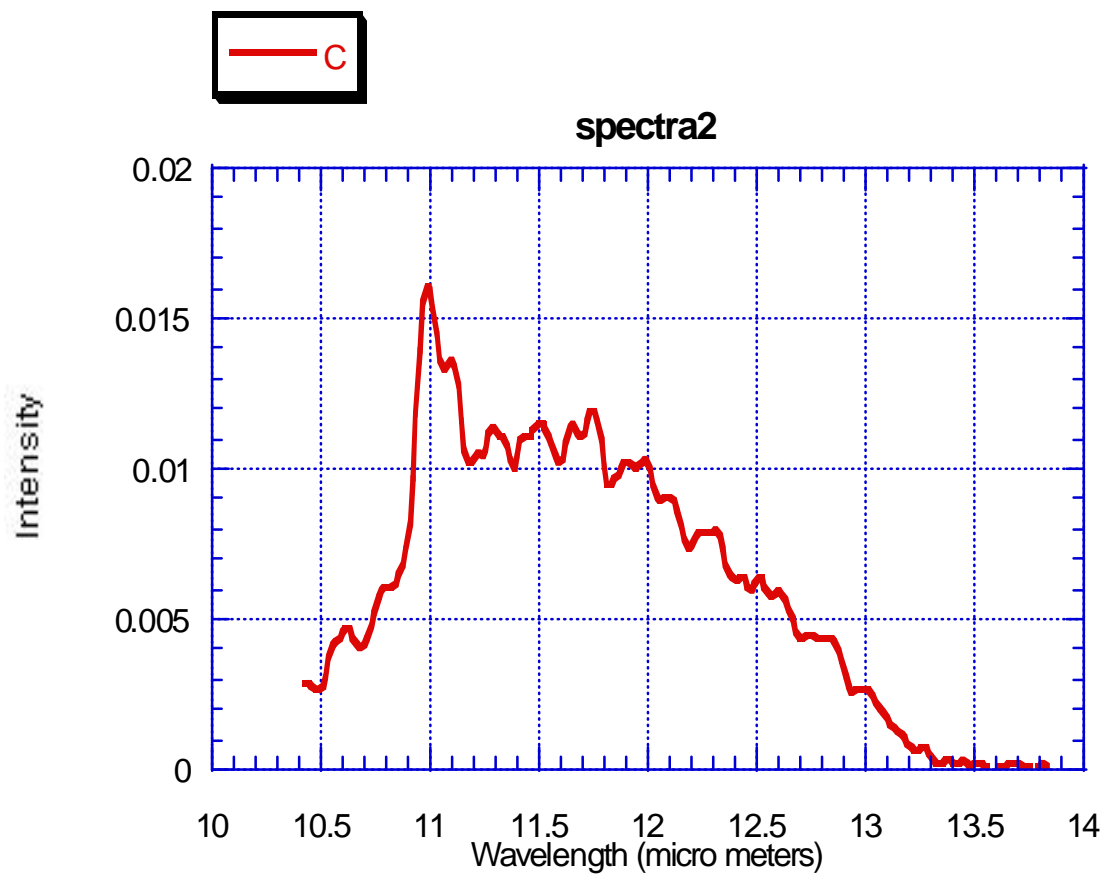
B. OPA Tuning

Data was taken in the form of intensity from a McPherson .3 meter scanning monochromator and wavelength that is converted from the stepper motor position. The data was plotted using Kaleidagraph and is displayed below. The monochromator's grating starting point was at 625 and the slit opening was 1mm. No filter was used. The shape of the plot was a surprise because it was not believed that the OPA system was tunable past 10 microns (10,000nm).



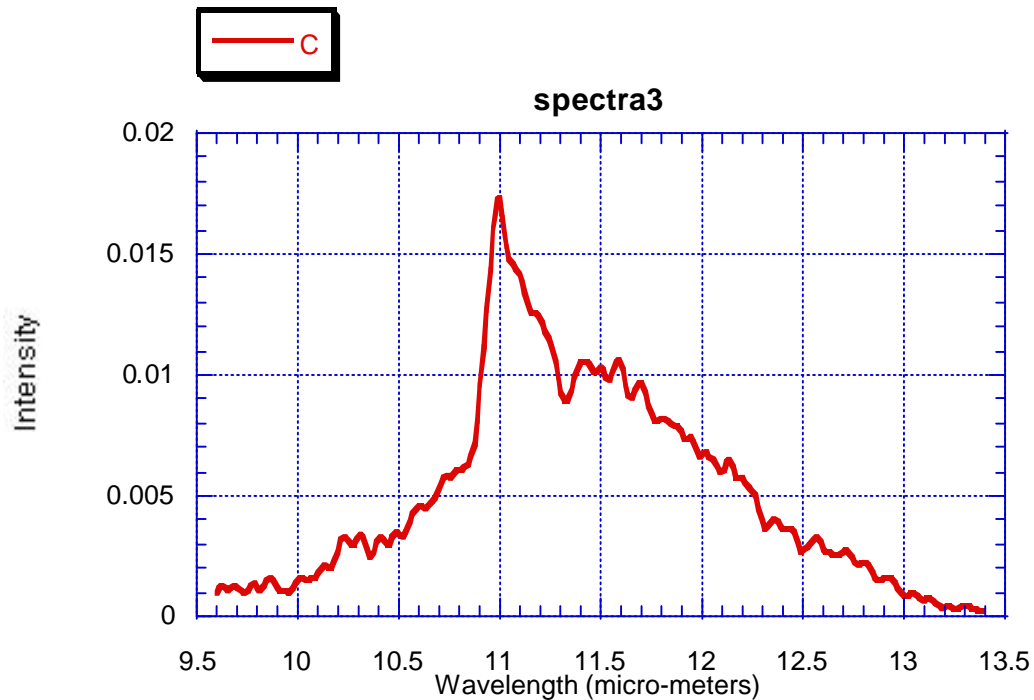
Spectra 1: BBO (35.02); DFM (9.53) notice the spike at 11

The spike at 11 microns was unexpected and was worth further investigation. We turned the BBO crystal to where we expected the OPA to output 11 micrometer light. The data is shown below. The monochromator's starting point was at 750 and the slit opening was 1.2mm. No filter was used.



Spectra 2: OPA reading: BBO (35.26); DFM(11.07)

Finally, we took another scan around 11 microns after tuning the OPA again. The monochromator's starting point was at 750 and the slit opening was 1mm. No filter was used.



Spectra 3 OPA reading: BBO (35.21); DFM (11.34)

We estimated from the graphs what the spectral width of these curves are and obtained for the three spectra: 1.6 microns, 1.4 microns, and 1.2 microns. To calculate the temporal width from the spectral width requires the two equations:

$$\nu = \frac{c}{\lambda} \quad (19)$$

$$\Delta\nu = \frac{c}{\lambda^2} \Delta\lambda \quad (20)$$

We let λ , which is designated by the center of the spectrum, be 10×10^{-6} m. The use of the uncertainty relation gives the temporal width:

$$\Delta t \geq 0.441 / \Delta \nu \quad (21)$$

For the spectral width 1.6 microns the temporal pulse width is estimated 91 femtoseconds. For the spectral width 1.4 microns the temporal width is estimated at 105 femtoseconds. For the spectral width 1.2 microns the temporal width is estimated at 122 femtoseconds.

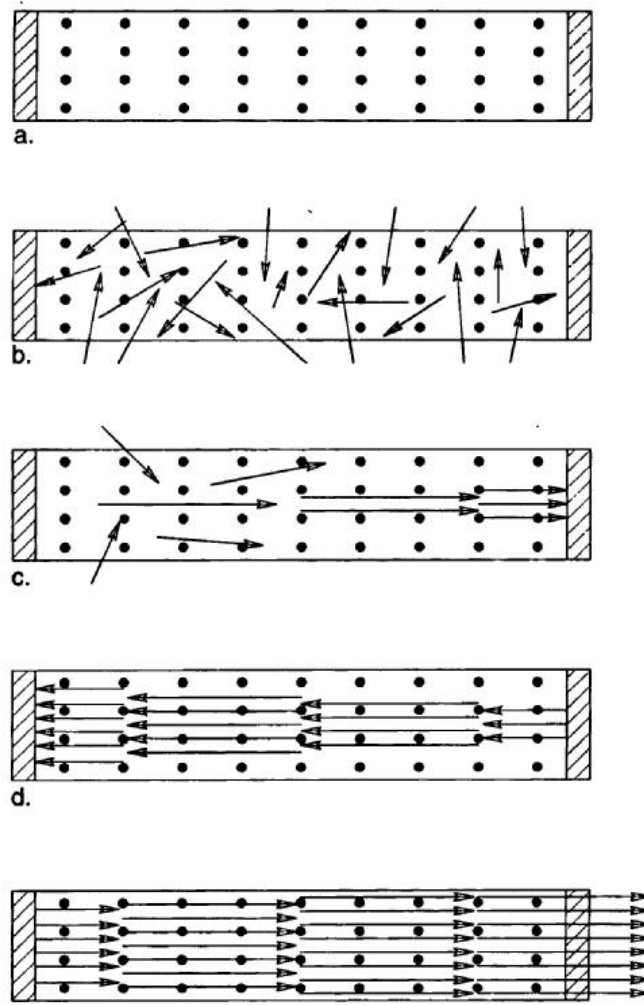
V. Conclusion

We have begun the characterization of an amplified Ti:Sapphire system and an OPA system. We attempted to measure the pulse width of the amplified beam before it went into the OPA and found a half-width value of 395 femtoseconds. This is much larger than the width of ~150 femtoseconds. The broadening may be due to an inappropriate optical equipment in our measurement setup.

The OPA system was not specified to be tuned past ten micrometers. However, we found that we did obtain decent spectra and light output past ten micrometers. We were surprised to observe any output from the system and even more surprised to see such a large spike in intensity at eleven micrometers. We estimated the spectral width of about 1.4 microns for the OPA spectra. This corresponds to the frequency range $\Delta\nu \sim 4 \times 10^{12}$ Hz. Using the uncertainty relation gives us a Δt greater than or equal to 110 femtoseconds. This is more like what is expected from the system, casting more doubt on our autocorrelation measurement. This work has begun the characterization of this laser system for experiments and has shown how easy it is to use this system.

VI Appendix

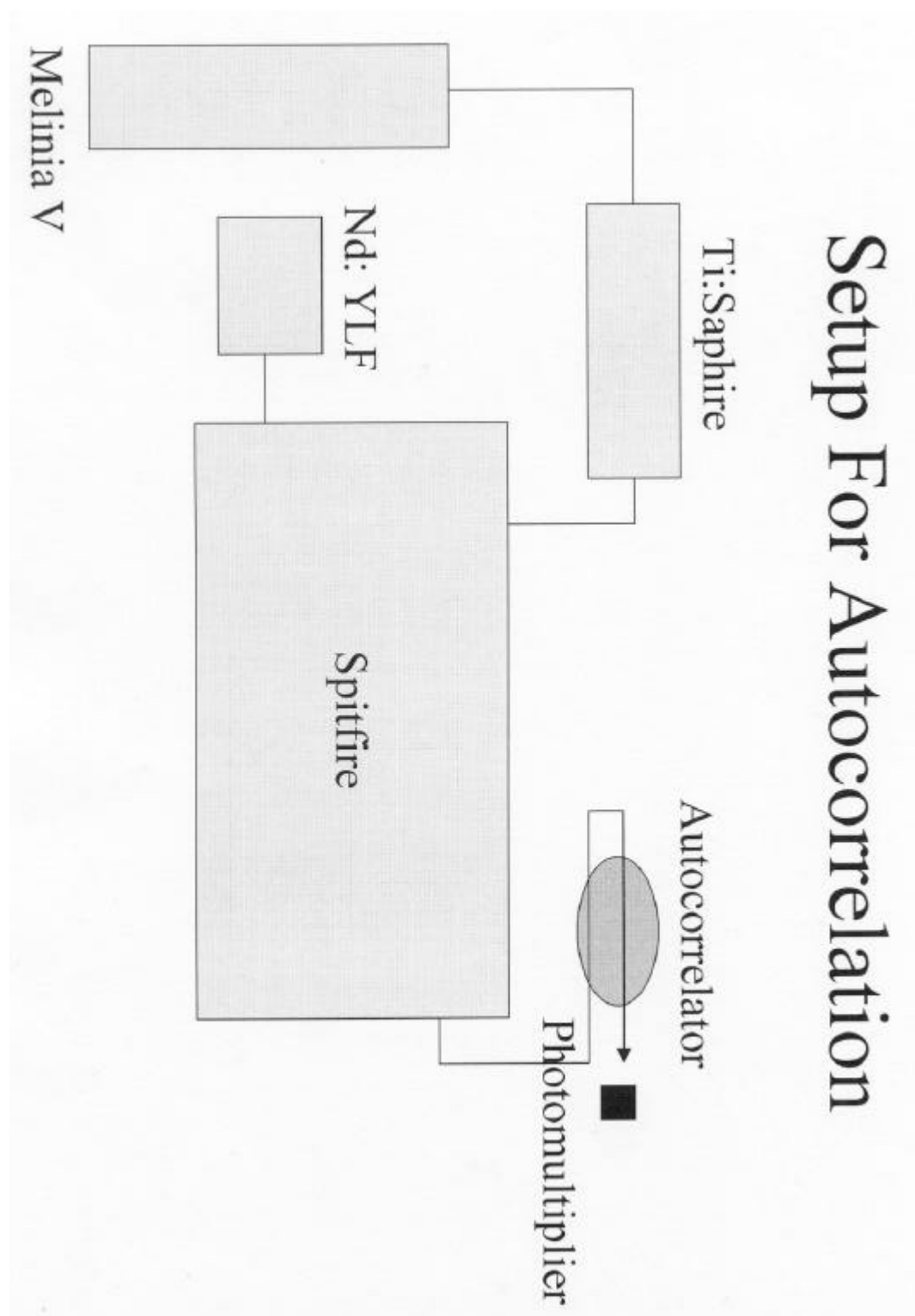
A. Appendix 1



Steps of a laser(taken from Reference 1)

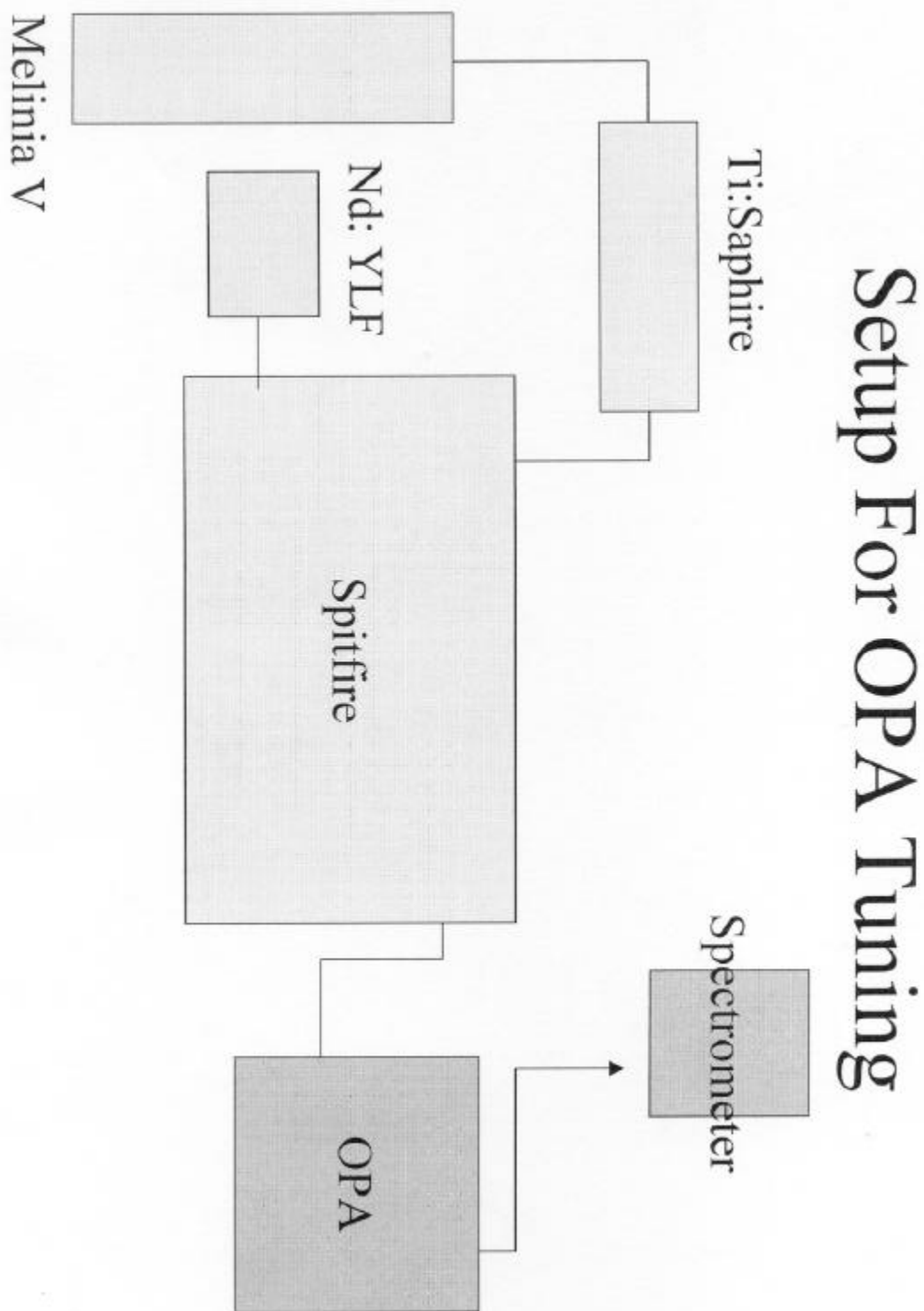
- a) The atoms begin at ground state
- b) Pumping light is introduced, depicted as black arrows
- c) An atom spontaneously emits a photon and the cascade begins
- d) This photon stimulates another atom to emit a photon and so on, this process continues as the photons are reflected back and forth between the ends of the crystal by mirrors
- e) The right hand end is only partially reflective and a constant wave is emitted

Appendix II



Melinia V pumps the Ti:Sapphire. The Ti:Sapphire beam is then amplified in the spitfire, which is being driven by a Nd:YLF laser. The amplified beam then enters an autocorrelation setup and is read by a photomultiplier.

Appendix III



Melinia V pumps the Ti:Sapphire. The Ti:Sapphire beam is then amplified in the spitfire, which is being driven by a Nd:YLF laser. The amplified beam then enters the OPA system and is read by a monochromator.

VII References

- [1] C.H. Townes, *How The Laser Happened*, New York: Oxford University Press, 1999.

- [2] J. Hecht, *Laser Pioneers*, Boston: Academic Press, Inc. 1992.

- [3] N. Bloembergen, *Nonlinear Optics*, 4th Edition, Singapore: World Scientific, 1996.

- [4] A. Einstein, *The Collected Papers of Albert Einstein/John Stachel, editor*. Princeton, N.J.: Princeton University Press, 1987.

- [5] B.B. Laud, *Lasers and Non-Linear Optics*, New York: Wiley, 1991.

- [6] A.E. Siegman, *Lasers*, Mill Valley, California: University Science Books, 1986.

- [7] R.W. Boyd, *Nonlinear Optics*, Boston: Academic Press, Inc. 1992

- [8] Y.P. Svirko, N.I. Zheludev, *Polarization of Light in Nonlinear Optics*, Chichester: John Wiley & Sons, 1998.

- [9] R.L. Sutherland, *Handbook of Nonlinear Optics*, New York: Marcel Dekker, 1996.
- [10] P. Yeh, *Introduction to Photorefractive Nonlinear Optics*. New York: John Wiley & Sons Inc. 1993.
- [11] C. Rulliere, *Femtosecond Laser Pulses Principles and Experiments*, New York: Springer, 1998.